Journal of Orthopaedic Translation 44 (2024) 125–138

Contents lists available at ScienceDirect

Journal of Orthopaedic Translation

journal homepage: www.journals.elsevier.com/journal-of-orthopaedic-translation

G protein-coupled receptor 30 activation inhibits ferroptosis and protects chondrocytes against osteoarthritis

Zhen Zhao [a,1], Shun Niu [a,1], Jun Chen [b,1], Hongtao Zhang [a], Lizuo Liang [a], Kui Xu [a], Chuan Dong [a], Chang Su [c], Tao Yan [c], Yongqiang Zhang [c], Hua Long [a,**], Le Yang [c,*], Minggao Zhao [c,***]

[a] Department of Orthopedics, Tangdu Hospital, The Air Force Medical University, Xi'an, Shaanxi, China
[b] Department of Osteology, Xi'an People's Hospital (Xi'an No. 4 Hospital), Xi'an, 710100, China
[c] Department of Pharmacy, Tangdu Hospital, The Air Force Medical University, Xi'an, Shaanxi, China

ARTICLE INFO

Keywords:
Ferroptosis
G-coupled protein receptor
Joints
Oestrogen
Osteoarthrosis
Yes-associated protein 1

ABSTRACT

Background: Osteoarthritis (OA) is the most common joint disease worldwide, but its cause remains unclear. Oestrogen protects against OA, but its clinical use is limited. G protein-coupled receptor 30 (GPR30) is a receptor that binds oestrogen, and GPR30 treatment has benefitted patients with some degenerative diseases. However, its effects on OA prevention and treatment remain unclear. Moreover, several studies have found that activation of estrogen receptors exerting anti-ferroptosis effects, which plays an important role in chondrocyte survival. Therefore, this study explored the general and ferroptosis-related effects and mechanisms of GPR30 in OA.

Methods: Genome-wide RNA sequencing, western blotting, and immunohistochemistry were used to evaluate GPR30 expression and ferroptosis-related indicators in cartilage tissues from clinical patients. Next, we investigated the effects of G1 (a GPR30 receptor agonist) on the function and pathology of OA in an animal model. We also treated chondrocytes with erastin (ferroptosis agonist) plus G1, G15 (GPR30 receptor antagonist), GPR30 short hairpin RNA, or ferrostatin-1 (ferroptosis inhibitor), then measured cell viability and ferroptosis-related indices and performed proteomics analyses. Finally, western blotting and reverse transcription-polymerase chain reaction were used to assess the effects of G1 on yes-associated protein 1 (YAP1) and ferritin heavy chain 1 (FTH1) expression.

Results: GPR30 expression was lower in the OA cartilage tissues than in the normal tissues, and G1 treatment significantly improved the locomotor ability of mice. Moreover, chondrocyte cell viability significantly decreased after erastin treatment, but G1 treatment concentration-dependently mitigated this effect. Furthermore, G1 treatment decreased phosphorylated YAP1 expression, increased activated YAP1 expression, and increased FTH1 transcription and protein expression, protecting against ferroptosis.

Conclusion: GPR30 activation inhibited ferroptosis in chondrocytes by suppressing YAP1 phosphorylation, which regulates FTH1 expression.

The Translational Potential of this Article: These results provide a novel potential target for therapeutic OA interventions.

1. Introduction

Osteoarthritis (OA), the most common joint disease worldwide, is the progressive degeneration of articular cartilage. OA causes pain, which leads to the loss of joint mobility and function, lifestyle limitations, and, ultimately, poor quality of life [1]. OA is characterised by pain, progressive articular cartilage degeneration, synovial inflammation, and subchondral bone changes, which cause joint destruction [2]. OA has

* Corresponding author.s
** Corresponding author.
*** Corresponding author.
E-mail addresses: tdlonghua@fmmu.edu.cn (H. Long), yanglefmmu@163.com (L. Yang), minggao@fmmu.edu.cn (M. Zhao).
[1] These authors contributed the same to this research.

https://doi.org/10.1016/j.jot.2023.12.003
Received 21 September 2023; Received in revised form 12 December 2023; Accepted 16 December 2023

several risk factors, including menopause, which is a major contributor to its pathogenesis [3]. Epidemiologic studies have reported that OA affects 18 % of women over the age of 60 years and that postmenopausal women have a rapidly increasing risk of OA compared to premenopausal women and men of the same age [4]. Therefore, the consensus is that oestrogen levels are key in OA development.

Oestrogen is an important regulator of chondrocyte function; it increases the synthesis of cartilage matrix-specific component aggregates and type II collagen and decreases the expression of inflammatory and catabolic genes [5]. However, oestrogen replacement therapy increases the risk of reproductive malignancies in female patients [6]; therefore, its use in clinical practice is limited. Articular cartilage is an oestrogen-sensitive tissue that expresses the classical nuclear oestrogen receptors (ER), ER-α and ER-β, and the novel oestrogen membrane receptor, G protein-coupled receptor 30 (GPR30), which belongs to the G protein-coupled receptor family. Moreover, GPR30 binds to oestrogen, mediating rapid non-genomic and genomic transcriptional responses to oestrogen, circumventing the side effects of oestrogen [7]. Currently, the protective role of GPR30 in degenerative and inflammatory diseases has been extensively studied [8,9]. However, although GPR30 is commonly expressed in osteoblasts and chondrocytes [10], few studies have examined its effects on the skeletal system and joint health.

Articular cartilage degeneration has been attributed to many causes, such as chondrocyte and necrotic apoptosis. However, recent studies suggest that ferroptosis may play a more important role [11]. Ferroptosis is a relatively newly discovered type of cell death induced by excess iron ions and reactive oxygen species (ROS) and driven by lipid peroxidation. Iron is a micronutrient critical for cell function and fate; however, excess iron increases ROS production through the Fenton reaction [12], and ROS overproduction damages DNA, proteins, and lipids, leading to ferroptosis. Ferroptosis involves antagonism between intracellular oxidative stress and antioxidant defence systems, and cellular oxidative stress injury is induced when iron accumulation greatly exceeds the antioxidant buffering capacity provided by cellular defenses [13]. Iron overload is common in the tissues of older adults, and ferroptosis plays an important role in the development of chronic diseases. Recent studies have shown that ferroptosis, characterised by the lethal accumulation of reactive iron and lipid peroxide, contributes to degenerative orthopaedic diseases [14], but ER exerts an anti-ferroptosis effect [15].

The role of GPR30 in ferroptosis has not been investigated, and the relationship between GPR30 expression and OA remains unclear. Therefore, this study explored the effects and mechanisms of GPR30 in OA to clarify its role and investigate its potential as a therapeutic target for OA treatment.

2. Materials and methods

2.1. Patients and specimens

Knee specimens were obtained from 15 patients with knee OA who underwent knee replacement surgery. The cartilage tissue was divided into an injury zone (designed for OA) and a corresponding undamaged zone (designed for Control). All human studies were approved by the Ethics Committee of the Second Affiliated Hospital of the Air Force Military Medical University (Assigned Number: TDLL-202309-06), and written informed consent was obtained before surgery. All experiments described were performed in accordance with the ethical guidelines of the World Medical Association (Declaration of Helsinki).

2.2. Animals

In this study, 20 8-week-old male C57BL/6 mice were used. All mice were anesthetized by intraperitoneal injection of pentobarbital sodium (35 mg/kg). Ten mice were randomly assigned to sham-operated groups. A destabilized medial meniscus (DMM) OA model was then established in 10 mice. The sham-operated group was randomly divided into two groups (5 mice per group): SHAM group and G1 (40 μg/kg/d) group, and DMM mice were randomly divided into two groups (5 mice per group): DMM + vehicle (saline) group and DMM + G1 (40 μg/kg/d) group. Equal amounts of lysate were injected intra-articularly in the sham-operated and DMM groups. Injections were started two weeks after surgery and continued every other day for 6 weeks. After 8 weeks, the mice were killed, and the right knee joint was removed and fixed in 4 % paraformaldehyde (PFA) for further experiments. All experimental procedures were approved by the Ethics Committee of the Fourth Military Medical University (approval reference number KY20193145) in full compliance with the ethical guidelines of the National Institutes of Health for the care and use of laboratory animals.

2.3. Isolation and culture of chondrocytes

Primary chondrocytes were isolated from cartilage tissue of the femoral condyle and tibial plateau of human knee joints removed from knee replacements. Briefly, the articular cartilage was first cut into small pieces and digested with 0.25 % trypsin for 30 min at 37 °C. After three washes with PBS, the cells were digested with 0.25 % type II collagenase (Sigma–Aldrich)at 37 °C for 8 h. The cell suspension was filtered through a 70 mm filter and centrifuged at 1000 rpm for 5 min to collect primary chondrocytes. Cells were cultured in DMEM/F12 (Gibco) supplemented with 10 % fetal bovine serum (Gibco) and 1 % penicillin/streptomycin. For our study, we used 3rd generation chondrocytes. ATDC5 cells were cultured in DMEM/F12 containing 10 % fetal bovine serum, and the ATDC5 cell line was validated by STR mapping. All cells were incubated at 37 °C in a humidified incubator containing 5 % CO2.

2.4. Knockdown of GPR30,FTH1 and YAP1 in ATDC5 cells

ShRNA sequences were designed based on previously reported sequences of GPR30 (Hsieh et al., 2007) [16]. The sense strand sequences of the GPR30, ferritin heavy chain 1 (FTH1) and yes-associated protein 1 (YAP1) shRNA can be found in Supplementary Table S1. Negative control shRNA was purchased from OBiO Technology (Shanghai) Corp., Ltd. Cells were transfected with lentivirus for 24 h according to the manufacturer's instructions. Staining was photographed at 96 h and analysed using fluorescence microscope (NIKON N1).

2.5. Histology and immunohistochemical assay

Tissues were fixed in 4 % paraformaldehyde, decalcified in 10 % EDTA solution for 2 weeks, and embedded in paraffin. Specimens were sectioned sagittally at 5 μm thickness and then stained with Safranin O/fast green. The severity of articular cartilage degeneration was evaluated using the OARSI scoring system. Immunohistochemistry (IHC): Sections were deparaffinized, antigen retrieved and then treated with 3 % H2O2. Non-specific binding sites were blocked with 10 % bovine serum albumin for 1 h at room temperature. Sections were incubated with anti-GPX4 (UK, ab125066, diluted 1:250), anti-GPR30(UK, ab260033, diluted 1:200), or anti-4-HNE (UK, ab48506, diluted 1:25) antibodies, followed by incubation with goat anti-rabbit secondary antibody. Then sections were stained with DAB and counterstained with hematoxylin. Images were captured with a fluorescence microscope and the number of positive cells in each group was counted under a 200× objective.

2.6. Cell viability assay

Chondrocyte activity was detected with Cell Counting Kit-8 (CCK-8) (EnoGene, Nanjing, China). Chondrocytes were inoculated into 96-well plates at a density of 5000 cells/well, apposed for 24 h and cultured with erastin to simulate cell death in OA. Chondrocytes were treated with G1, Ferrostatin-1 (Fer-1), Necrostatin-1 (Nec-1) and Z-VAD-FMK (Beyotime) to rescue cell death. 100 μL of 10 % CCK-8 solution was added to each

well, incubated for 2 h at 37 °C off light, and absorbance was measured at 450 nm.

2.7. Western blot analysis

Cells and homogenized cartilage tissue were lysed with RIPA lysis buffer (Beyotime, Shanghai, China), separated by 12 % polyacrylamide gel electrophoresis (PAGE), and transferred to PVDF membranes. PVDF membranes were incubated with primary antibodies overnight at 4 °C and with secondary antibodies for 1 h at room temperature and visualized using the Chemiluminescence Imaging System. The density of each band was quantified using Image J version 1.48. The antibodies can be found in Supplementary Table S2.

2.8. Iron ion detection in cartilage and synovial fluid

The Ferrous Iron Colorimetric Assay Kit (Elabscience, E-BC-K773-M) was used to detect the ferrous ion content of articular cartilage and synovial fluid according to the manufacturer's instructions. Briefly, 100 mg of fresh human cartilage tissue was placed in a sterile test tube containing 1 mL of assay buffer, homogenized on ice at 4 °C, and the homogenate was centrifuged at 10,000×*g* for 10 min, and the supernatant was collected. After incubation at 37 °C for 10 min, the absorbance was measured by microplate reader at 593 nm, and then the Fe^{2+} levels of cartilage and synovial fluid were calculated.

2.9. Detection of intracellular ROS and lipid-ROS

Chondrocytes and ATDC5 cells were inoculated into 6-well plates at a density of 4×10^5 cells/well. After 24h, 1 μmol or 10 μmol erastin with 1 μM G1 or 1 μM ferrostain-1 was added for 24h. Intracellular ROS and lipid ROS levels were detected by fluorescence microscopy and flow cytometry using DCFH-DA (Jiancheng , Nanjing , CHINA) and Liperfluo fluorescent probes (Dojindo , Kumamoto , JAPAN) . Briefly, chondrocytes were washed 3 times with PBS and then treated with 5 μM DCFH-DA or 1 μM Liperfluo for 30 min at 37 °C in the dark. After incubation, cells were washed with PBS and detected by fluorescence microscopy and flow cytometry (excitation wavelength: 488 nm, emission wavelength: 500–550 nm).

2.10. Malondialdehyde (MDA) assay

Malondialdehyde levels were measured using the Lipid Peroxidation Malondialdehyde Assay Kit (Elabscience, E-BC-K028-M). Chondrocytes and ATDC5 cells were inoculated into 6-well plates. Cells were treated as described above for 24 h. Cells were transferred to centrifuge tubes, 0.5 mL of extraction solution was added, and cells were disrupted by ultrasonic fragmentation. 0.1 mL of sample or standard solution was added to 1 mL of malondialdehyde assay working solution, heated in a water bath at 100 °C for 40 min, cooled under running water to room temperature, and then centrifuged at 1000×*g* for 10 min at room temperature. The OD value at 532 nm was measured using the microplate reader, and the protein concentration was quantified to normalize the MDA content.

2.11. Mitochondrial membrane potential detection

Mitochondrial membrane potential was measured using the JC-1 Mitochondrial Membrane Potential Analysis Kit (Beyotime, C2006, China). Briefly, chondrocytes were inoculated into 6-well plates, cultured overnight, and treated as described above for 24 h. Cells were then incubated with 1 × JC-1 staining solution for 30 min at 37 °C in the dark and observed under the fluorescence microscope.

2.12. Intracellular Fe^{2+} levels

Chondrocytes were inoculated into 48-well plates. Cells were treated as described above for 24 h and then washed 3 times in HBSS. Cells were then stained with 1 μM FerroOrange (Dojindo, Kumamoto, Japan) at 37 °C, 5 % CO2 for 30 min and immediately imaged with the fluorescence microscope.

2.13. Paw withdrawal mechanical threshold test (PWMT)

The plantar automatic mechanical piercing instrument was purchased from Jiangsu Cylon Biotechnology Co., LTD (SA502). Briefly, the mechanical threshold of the hind paw was tested with a series of von Frey monofilaments ranging from 0.008 to 2.0 g (0.008, 0.02, 0.04, 0.07, 0.16, 0.4, 0.6, 1.0, 1.4, and 2.0 g). The experiment was started with a 0.008 g filament and the minimum force that elicited a positive response (licking, biting, and abrupt withdrawal of the hind paw) was recorded. All experiments were repeated 3 times, each time at 5 min intervals. To avoid diurnal variation, we performed all behavioral tests in the morning (9 AM–12 PM).

2.14. Open field test (OFT)

Mice tracking was analysed by using a video tracking system (VanBi Tracking Master V3.0, Shanghai Vanpen Intelligent Technology Co., Ltd.). Before the experiment, the mice were acclimated to the experimental environment for 3 h, and the experimental procedure was kept quiet. During the experiment, each mouse was placed in the centre area of the chamber and allowed to explore freely for 15 min. The exploration behaviour of the mice was recorded by a video camera mounted above the chamber.

2.15. Micro-CT analysis

Briefly, skin and muscle were removed to obtain the knee joint. The joint specimens were then fixed in 4 % PFA. All specimens were scanned with a small animal Micro CT (Quantum GX2, PerkinElmer, USA). The 3D images were visualized and further analysed using SimpleViewer (5.5.0.15) and 3-matic Research 13.0 (x64).

2.16. Quantitative reverse-transcription PCR

Total RNA from cells was extracted using TRIzol Reagent (Sangon Biotech), and complementary cDNA was synthesized by reverse transcription using cDNA synthesis kit (Invitrogen, CA). Detection of target gene expression on Light Cycler 480 (Roche) using FastStart Essential DNA Green Master (Roche) and expression levels were normalized to GAPDH.FTH1 primer sequences were: 5′- CAAGTGCGCCAGAACTACCA-3′. GAPDH primer sequences were: 5′-AGGTCGGTGTGAACGGATTTG-3′ (forward) and 5′-TGTAGACCATCTAGTTGAGGTCA-3′ (reverse). -3′ (reverse).

2.17. Immunofluorescence staining

Chondrocytes were inoculated into 24-well plates. After cell treatment, the cells were fixed with 4 % PFA for 15 min at room temperature. Chondrocytes were permeabilized with 0.5 % Triton X-100 for 20 min and then blocked with 5 % bovine serum albumin for 1 h at room temperature. Chondrocytes were incubated with YAP1 antibody overnight at 4 °C and with Cy3-conjugated goat anti-rabbit secondary antibody in the dark for 1 h on day 2. After washing three times with PBS, cells were incubated with DAPI for 5 min. Images were captured with a fluorescence microscope.

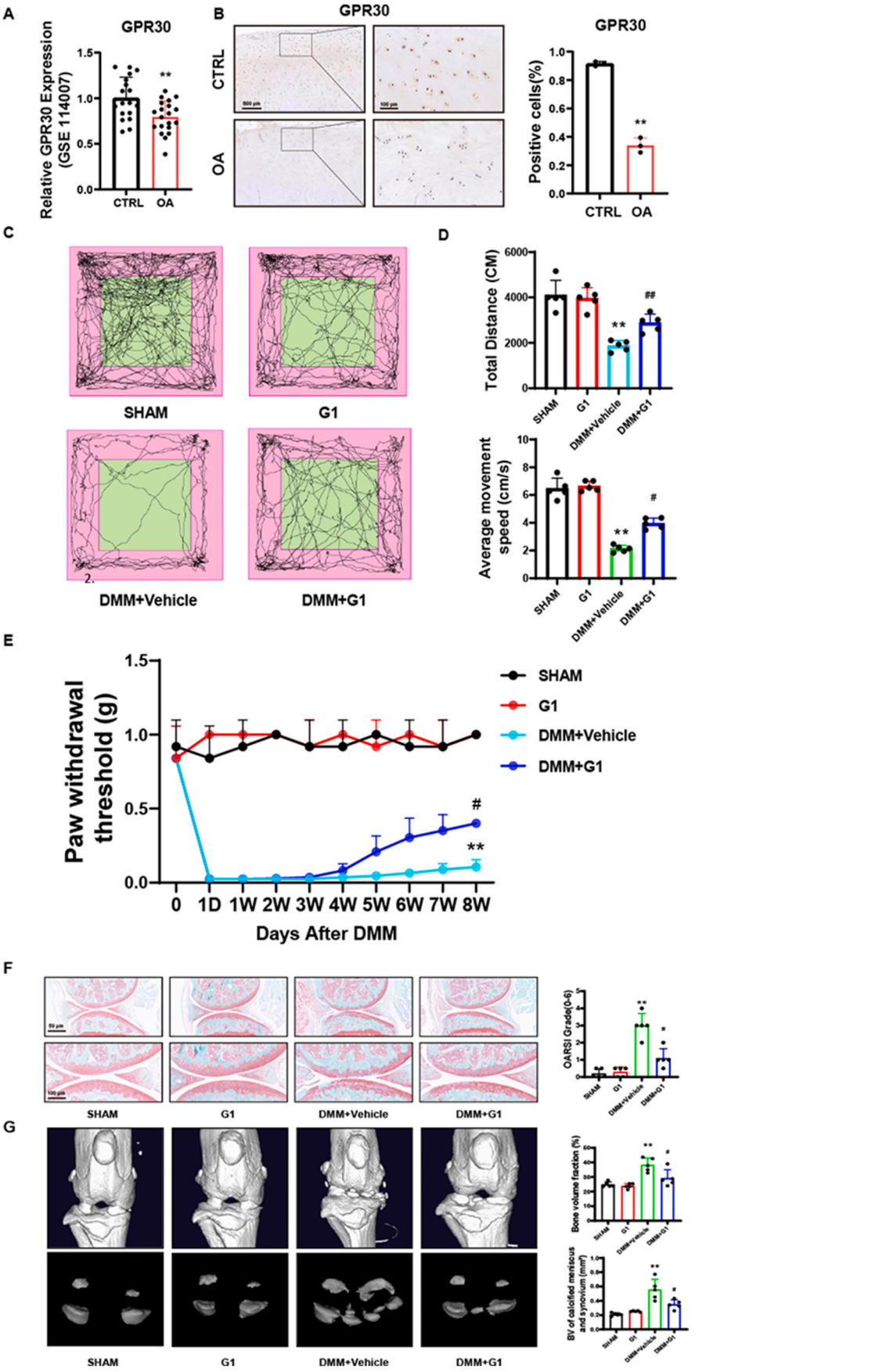

(caption on next page)

Figure 1. GPR30 expression was decreased in human osteoarthritic cartilage and GPR30 activation improved the symptoms of osteoarthritic mice (A) Genome-wide RNA-Seq data of GPR30 expression level of OA cartilage and undamaged cartilage. Date was originated from GSE114007. (B)Immunohistochemistry assay with anti-GPR30 in severely damaged and undamaged cartilage tissues (n = 3). (C)Open field test in OA mice models (n = 5). (D)The total distance and average movement speed in OA mice models (n = 5). (E) Paw withdrawal mechanical threshold test in OA mice models (n = 5). (F) Safranin O-fast green images of mice knee joints (n = 5). (G)Three-dimensional models of mice knee joints (n = 5). $^{*}P < 0.05$, $^{**}P < 0.01$ compared with sham group. $^{\#}P < 0.05$ compared with OA group. Error bars represent SD. (For interpretation of the references to colour in this figure legend, the reader is referred to the Web version of this article.)

2.18. Transmission electron microscopy of cartilage

Fresh mouse knee cartilage was harvested, frozen, and immediately cut into 1 mm^3 volumes. The cartilage tissue was then fixed in 2.5 % glutaraldehyde solution, followed by fixation in 1 % Osmium acid fixative and dehydration in ethanol and acetone. Specimens were prepared by overnight impregnation with a gradient of anhydrous acetone and epoxy resin, embedded in resin and polymerized at 60 °C for 48 h. The embedded specimens were sectioned using a Leica EM UC7 ultrathin cutter. Ultrathin sections were collected on copper mesh, stained with uranyl acetate and lead citrate, and observed with a transmission electron microscope (JEM-1400FLASH).

2.19. Statistical analysis

All data are expressed as mean ± standard error of the mean (SEM). Statistical analysis was performed using Prism GraphPad version 8.3.0. Differences between two groups of data were determined by Student's two-tailed t-test. Two-way ANOVA was used to determine differences between more than two groups. In all cases, $P < 0.05$ was considered statistically significant.

3. Results

3.1. GPR30 expression decreased in human osteoarthritic cartilage, and GPR30 activation significantly improved the symptoms of osteoarthritic mice

We used genome-wide RNA sequencing (GEO accession number: GSE114007) to explore GPR30 expression in human osteoarthritic cartilage tissues. The GPR30 transcript level was significantly lower in osteoarthritic cartilage tissues than in normal cartilage tissues (Fig. 1A). Furthermore, immunohistochemical staining and western blotting analyses of tissues from patients with OA demonstrated that GPR30 protein expression was significantly lower in severely damaged cartilage tissues than in undamaged cartilage tissues (Figs. 1B and 2F).

Next, we used medial meniscus destabilisation to establish an OA mouse model and verify the effects of GPR30 on OA prevention and treatment. Mice in the DMM group travelled a significantly shorter total distance and moved at a significantly slower speed than those in the control group in OFT. However, treatment with G1, a GPR30 receptor agonist, significantly improved the locomotor ability of the mice (Fig. 1C and D). Moreover, the mice were monitored for mechanical pain in the lower limb preoperatively, day one postoperatively, and then weekly for eight weeks after surgery. Significant hyperalgesia was observed in the DMM groups. However, after four weeks, nociception was significantly relieved in the DMM + G1 group compared to the DMM + Vehicle group. Pain reduction during the early postoperative period did not differ among the groups (Fig. 1E). Early postoperative pain is mainly due to surgery-inflicted injuries, whereas late-stage pain is primarily associated with OA. Thus, the results suggest that G1 exerted analgesic effects by slowing OA progression.

The mice were sacrificed eight weeks after DMM surgery, and histologic changes to the cartilage were evaluated by staining with safranin O/fast green. Articular cartilage destruction was apparent in the DMM + Vehicle group, but the OARSI score significantly improved in the DMM + G1 group compared to the DMM + Vehicle group (Fig. 1F). Similar results were observed for the relative bone volume fraction of the subchondral bone and the intra-articular bone flap volume, which were significantly higher after DMM surgery and significantly improved by G1 administration, indicating that G1 reduced the degree of subchondral bone sclerosis and intra-articular calcification (Fig. 1G). The above experiments demonstrated that GPR30 agonism participates in OA prevention and treatment in mice.

3.2. Ferroptosis is important in OA process, and activation of GPR30 reduced chondrocyte ferroptosis

A recent study found that ferroptosis may affect OA progression [17]. Thus, we explored the relationship between OA and chondrocyte ferroptosis. First, correlation analyses using genome-wide RNA sequencing data demonstrated that GPR30 expression in cartilage tissues negatively correlated with ferroptosis driver and marker genes and positively correlated with ferroptosis suppressor genes (Fig. 2A). Furthermore, glutathione peroxidase (GPX4) expression, a key ferroptosis regulator, was lower in osteoarthritic cartilage tissue than in normal cartilage tissue (Fig. 2B). Moreover, immunohistochemical staining and western blotting analyses of cartilage tissues from patients with OA demonstrated that GPX4 expression was lower in cartilage tissues with severe damage than in undamaged tissues (Fig. 2C–F). Furthermore, we collected joint fluid from patients undergoing arthroscopic explorations, finding that the Fe^{2+} content in the joint fluid of patients with OA was significantly higher than that in patients without OA. The Fe^{2+} content was also significantly higher in damaged cartilage tissue than in undamaged tissue (Fig. 2D). Finally, immunohistochemical staining revealed elevated 4-Hydroxynonenal (4-HNE) levels, a lipid peroxidation metabolite marker, in severely damaged cartilage tissues (Fig. 2E). These results suggest that ferroptosis plays an important role in OA development.

Next, we tested whether GPR30 has a protective effect against chondrocyte ferroptosis using erastin (a ferroptosis agonist) to simulate cellular ferroptosis. High erastin concentrations significantly decreased the viability of ATDC5 chondrocytes and human primary chondrocytes (Fig. 2G), but G1 administration concentration-dependently improved their viability (Fig. 2H). We also treated chondrocytes with G15 (a GPR30 receptor antagonist) and FER-1 (a ferroptosis inhibitor), finding that FER-1 elicited a protective effect, and G15 inhibited the protective effect of G1 treatment (Fig. 2I). Intriguingly, necrostatin-1 (a necroptosis inhibitor) and Z-VAD-FMK (a caspase inhibitor) administration did elicit protective effects on erastin-stimulated chondrocytes (Fig. 2J), suggesting that erastin does not act by enhancing apoptosis or necroptosis and that G1 exerts its protective effect primarily by inhibiting ferroptosis via GPR30 receptor antagonism.

3.3. GPR30 activation affected intracellular ferrous ions and ROS production in chondrocytes

Treatment with ferroptosis inducers in chondrocytes increased the intracellular free ferrous ion level, but G1 and FER-1 administration significantly decreased it (Fig. 3A). Increased ferrous ions increases ROS and lipid peroxide levels in cells, which we also observed. Treatment with ferroptosis inducers increased intracellular ROS and lipid peroxide levels, whereas G1 and FER-1 treatment decreased their production (Fig. 3B and C). We also measured the intracellular malondialdehyde (MDA) concentration, a lipid peroxidation metabolite, finding results consistent with those of the lipid peroxidation assay (Fig. 3E). Finally,

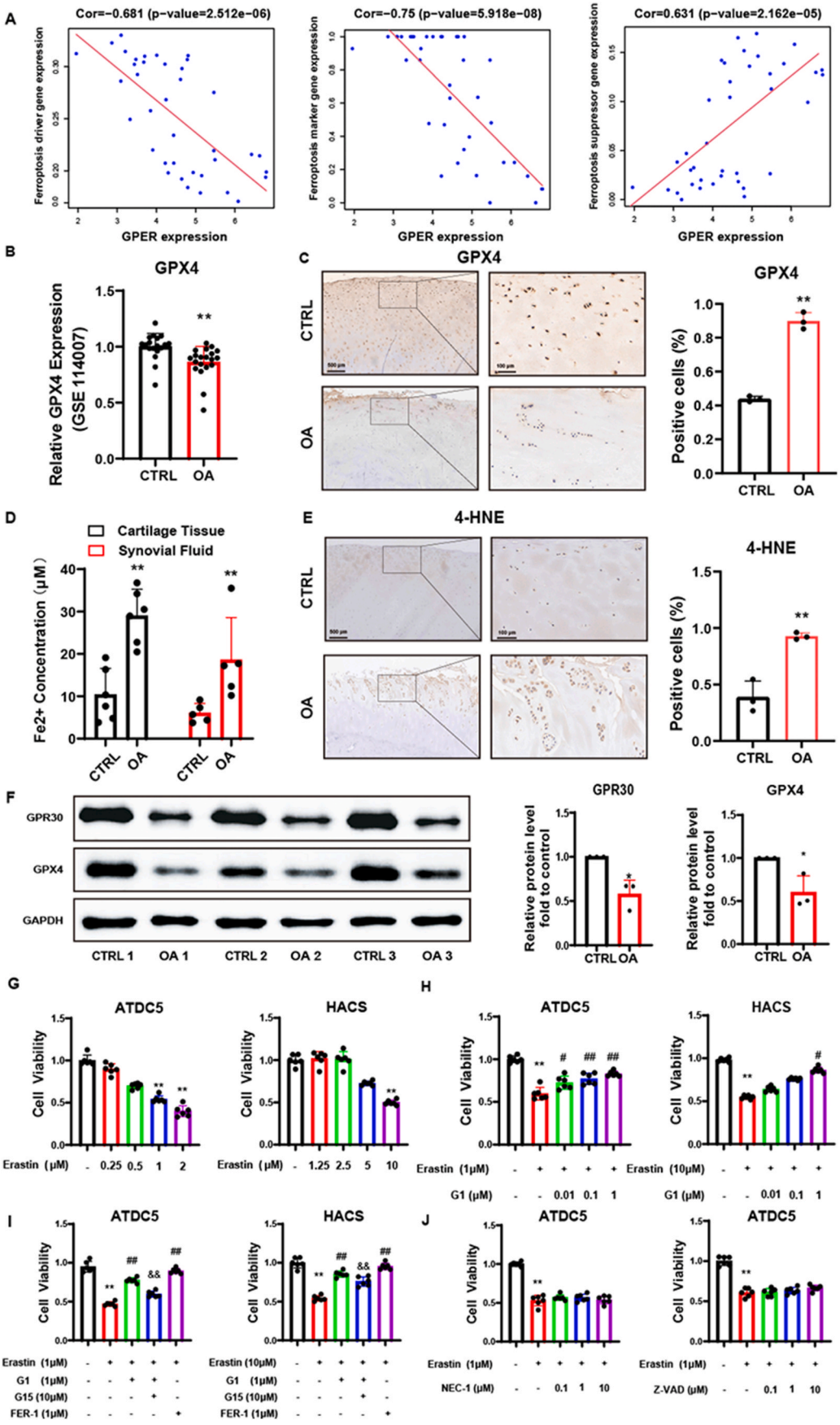

(caption on next page)

Figure 2. Activation of GPR30 reduced chondrocyte ferroptosis. (A) Correlation of GPR30 with ferroptosis using whole genome RNA sequencing data. (B) Genome-wide RNA-Seq data of GPX4 expression level of OA cartilage and undamaged cartilage. Date was originated from GSE114007. (C) Immunohistochemistry assay with anti-GPX4 in severely damaged and undamaged cartilage tissues (n = 3). (D) Fe^{2+} in OA cartilage and corresponding non-lesion cartilage tissues (n = 5) and Fe^{2+} in OA and normal synovial fluid (n = 5). (E) Immunohistochemistry assay with anti-4HNE in severely damaged and undamaged cartilage tissues (n = 3). (F) Protein expression of GPR30 and GPX4 of OA cartilage and undamaged cartilage analysed by Western blot (n = 3). (G) Cell viability of ATDC5 cells and HACS treated with different concentration of erastin for 24 h measure by CCK8 (n = 6). (H) Cell viability of ATDC5 cells and HACS treated with erastin and rescued via different concentration of G-1 for 24 h measure by CCK8 (n = 6). (I) Cell viability of ATDC5 cells and HACS treated with erastin and rescued via G1, G15 and Fer-1 for 24 h measure by CCK8 (n = 6). (J) Cell viability of ATDC5 cells and HACS treated with erastin and rescued via Nec-1 and Z-VAD for 24 h measure by CCK8 (n = 6). $^{*}P < 0.05$, $^{**}P < 0.01$ compared with control group. $^{\#}P < 0.05$, $^{\#\#}P < 0.01$ compared with erastin group. $^{\&\&}P < 0.05$ compared with erastin + G1 group. Error bars represent SD.

mitochondrial damage is another manifestation of cellular ferroptosis, and we found that G1 treatment restored the chondrocyte mitochondrial membrane potential (Fig. 3F).

3.4. GPR30 activation increased FTH1 expression levels

We also sequenced erastin- and erastin + G1-treated chondrocytes and performed proteomic analyses to investigate the mechanism of G1 protection against ferroptosis. We identified 168 differentially expressed proteins between the erastin and erastin + G1 groups; 92 genes were upregulated, and 76 genes were downregulated (Fig. 4A).

In the GO analysis, the differentially expressed proteins were mainly associated with iron ion metabolism (Fig. 4B). In the KEGG pathway analysis, the differentially expressed proteins were mainly enriched in the ferroptosis pathway, demonstrating that G1 acts mainly by inhibiting ferroptosis (Fig. 4C). The Hippo pathway was also enriched (Fig. 4C), consistent with the results of Liang C and Gao R et al., who reported that the Hippo pathway is important in ferroptosis [18,19]. Furthermore, Aliagan et al. found that GPR30 activation helps protect the Hippo pathway against oxidative stress [20], indicating that the Hippo pathway may play an important role in the anti-ferroptosis effect of G1.

We also performed a PPI network analysis, finding that the most significantly upregulated protein in the ferroptosis pathway was FTH1 (Fig. 4D), consistent with the positive correlation between GPR30 expression and FTH1 in the GSE114007 dataset , meanwhile, CP and FLT proteins were negatively correlated or not correlated with GPR30 expression(Fig. 4E and F). Ferritin is a protein commonly expressed by cells, and FTH1 catalyses the first step of ferric ion storage in the Fe^{2+} oxidation reaction, inhibiting the Fenton reaction and suppressing ferroptosis [20]. Interestingly, Qu et al. found that GPR30 receptor activation increases FTH1 protein expression [22], and Zhou et al. reported that FTH1 transcript levels were affected by the regulation of the Hippo pathway, specifically by the core regulator YAP1 [23].

These results indicate that FTH could be essential to GPR30's protective effect against ferroptosis and that GPR30 might regulate FTH1 expression levels via the Hippo signalling pathway.

3.5. GPR30 activation exerted anti-ferroptosis effects by increasing FTH1 expression

Next, we performed western blotting to confirm if GPR30 exerts its protective effect against ferroptosis in chondrocytes by regulating FTH1. Erastin treatment reduced FTH1 and GPX4 protein expression in chondrocytes, but G1 treatment significantly increased their expression. However, dihydroorotate dehydrogenase (DHODH) and cystine/glutamate antiporter SLC7A11(i.e. xCT) (ferroptosis regulatory proteins) were not affected (Fig. 5A and B).

Furthermore, GPR30 knockdown in ATDC5 chondrocytes using GPR30-specific short hairpin RNA simultaneously downregulated FTH1 expression but did not affect GPX4 expression (Fig. 5C). Cell viability also significantly decreased in GPR30 knockdown at the same concentration of erastin (Fig. 5D), indicating that the GPR30 knockdown cells were more sensitive to ferroptosis, correlating with low FTH1 expression. Finally, we knocked down FTH1 and found that the protective effect of G1 against ferroptosis was significantly diminished (Fig. 5E and F). Thus, GPR30 reduced lipid peroxide production by increasing FTH1 levels and stabilising intracellular iron pools, which led to GPX4 inactivation and, thus, anti-ferroptosis effects.

3.6. GPR30 activation inhibited YAP1 phosphorylation to regulate FTH1 transcription and protect against ferroptosis

The proteomic analysis suggested that GPR30 exerts its anti-ferroptosis effects through the Hippo signalling pathway. Therefore, we investigated the effects of G1 on YAP1 expression, a core Hippo signalling pathway regulator. Erastin treatment decreased activated YAP1 expression. G1 treatment decreased the phosphorylated YAP1 level but increased the activated YAP1 protein level (Fig. 6A) and the nuclear shift of YAP1 (Fig. 6B). We also found that the YAP1 inhibitor, verteporfin, concentration-dependently decreased the protective effects of G1 against chondrocyte ferroptosis (Fig. 6C). Verteporfin also inhibited FTH1 transcription and protein expression levels (Fig. 6D and E). Finally, we knocked down YAP1, which significantly attenuated the protective effect of G1 against ferroptosis (Fig. 6E and F). These results suggest that GPR30 regulates FTH1 transcription to protect against ferroptosis by altering the YAP1 phosphorylation level.

3.7. GPR30 activation inhibited ferroptosis and slowed down OA progression in mice

Transmission electron microscopy analysis of chondrocytes isolated from the OA mouse model identified morphological changes in the mitochondria, which are characteristic ferroptosis alterations. An ultrastructural analysis showed that mitochondrial ridges were reduced or absent, and the mitochondria were swollen in the osteoarthritic chondrocytes. However, G1 treatment prevented these ultrastructural and morphological changes (Fig. 7A). Finally, immunohistochemical staining showed that chondrocyte 4-HNE expression in mouse cartilage tissue was significantly higher after DMM surgery than SHAM group, similar to the human cartilage tissue. Moreover, G1 treatment significantly reduced chondrocyte 4-HNE expression and increased FTH1 expression compared to the vehicle group, indicating that G1 reduced the occurrence of chondrocyte ferroptosis in mice after DMM surgery by increasing FTH1 expression in chondrocytes (Fig. 7B). These in vivo results suggest that G1 protects against OA progression by inhibiting ferroptosis.

4. Discussion

This study aimed to elucidate the anti-ferroptosis role of the GPR30 in OA. We found significantly lower GPR30 expression in osteoarthritic cartilage than in normal cartilage. We also found evidence that ferroptosis is essential to OA and that GPR30 is closely associated with ferroptosis. Moreover, GPR30 agonism inhibited YAP1 phosphorylation and increased activated YAP expression, which increased FTH1 transcription, subsequently inhibiting chondrocyte ferroptosis by increasing FTH1 expression, thus mitigating the progression and occurrence of OA.

Oestrogen is important for the status of joints. For instance, Xiao et al. reported that oestrogen reduces pain in patients with OA [24]. Similarly, our in vitro experiments demonstrated that GPR30 agonists

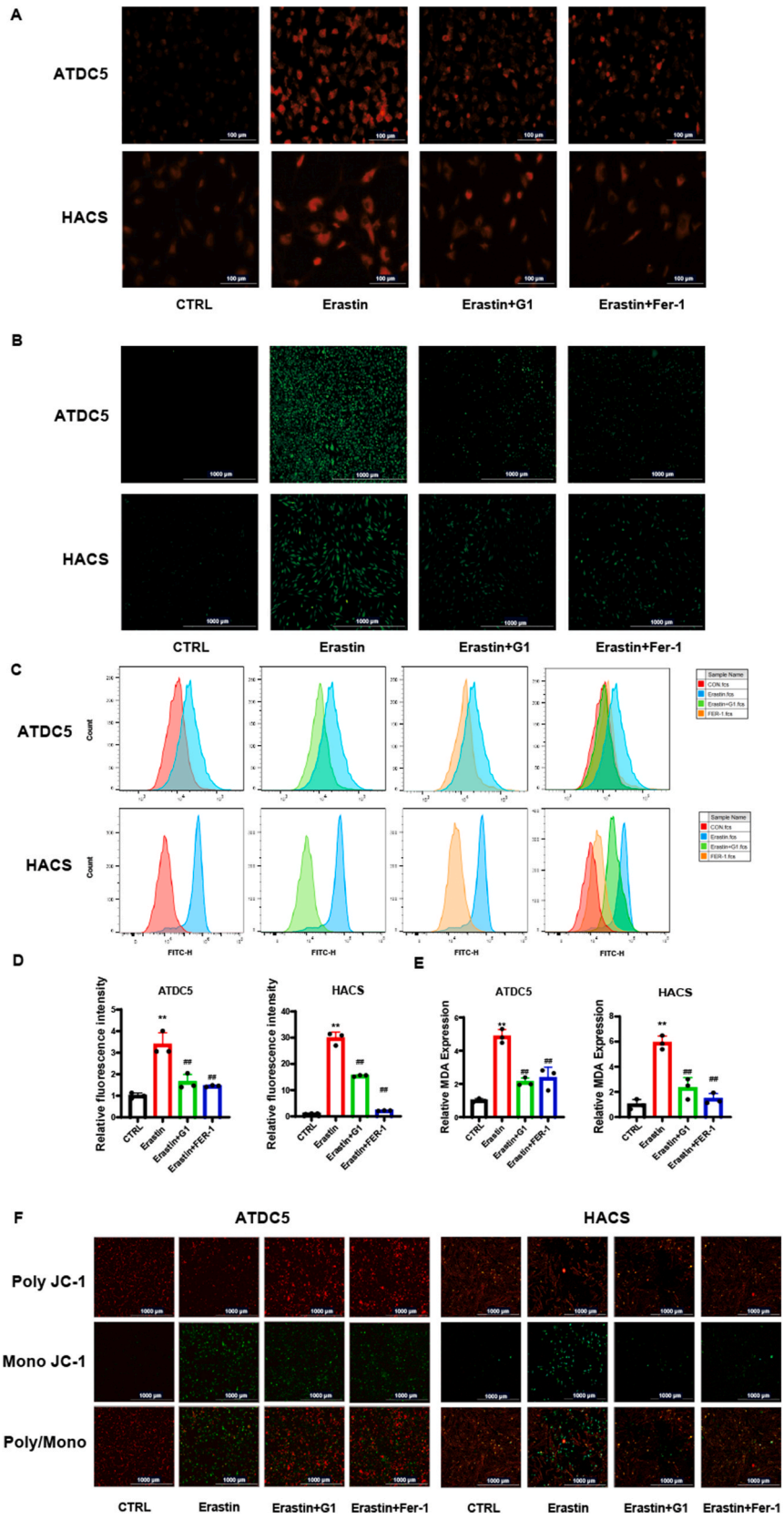

Figure 3. GPR30 activation affected intracellular ferrous ions and ROS production in chondrocytes. (A) Intracellular Fe^{2+} level (B) ROS level (C) Lipid ROS level (E) MDA level and (F) Mitochondrial membrane potential was analysed in ATDC5 cells and HACS treated with erastin and rescued via G1 and Fer-1 for 24 h (n = 3). $^{**}P < 0.01$ compared with control group. $^{\#\#}P < 0.01$ compared with erastin group. Error bars represent SD.

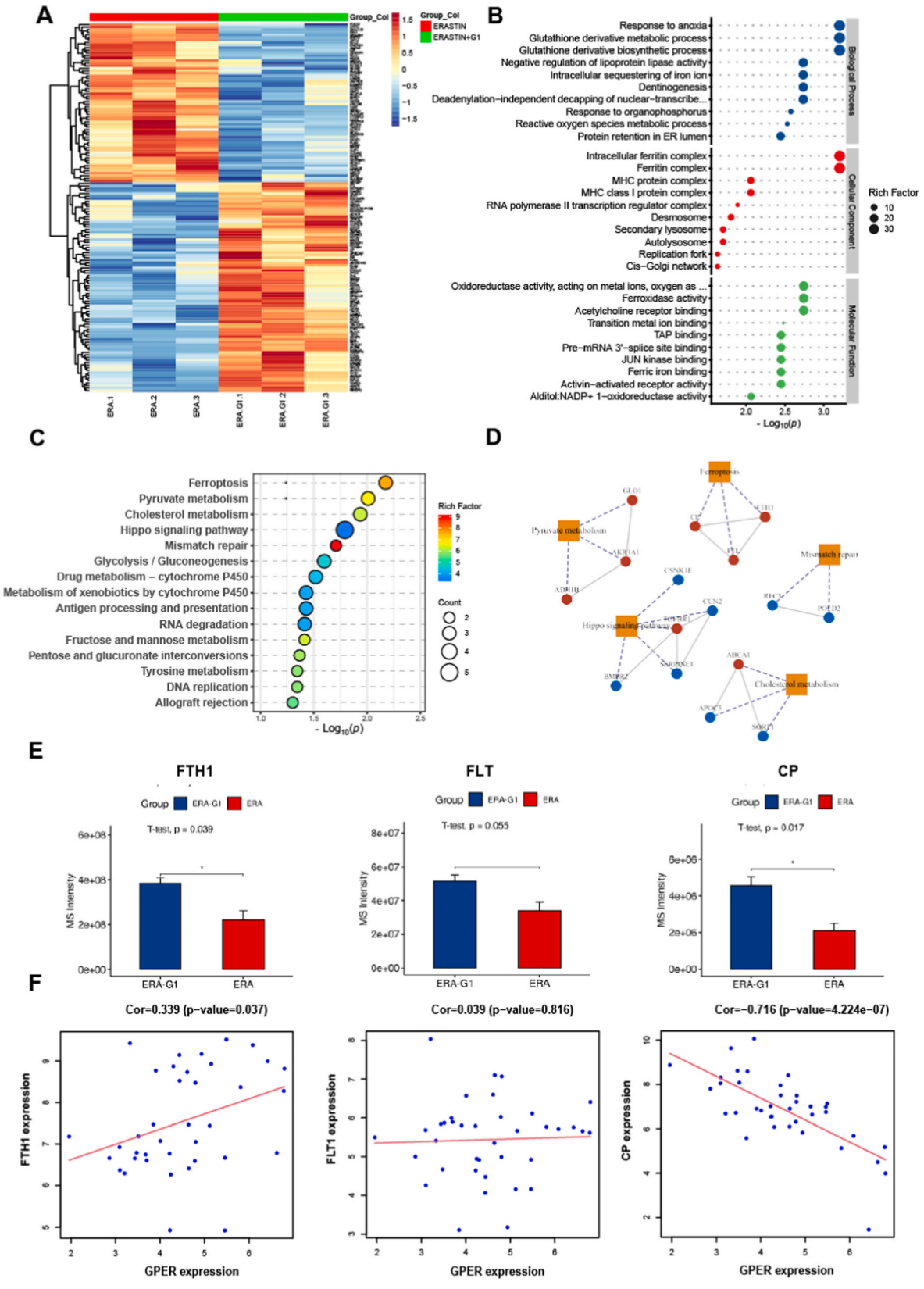

Figure 4. GPR30 activation increased FTH1 expression levels. (A) A heat map illustrating differentially regulated gene expression from proteomic analysis between erastin and erastin + G1 groups HACS (B) Gene ontology (GO) analysis (C) Kyoto Encyclopedia of Genes and Genomes (KEGG) analysis (D) PPI network analysis between erastin and erastin + G1 groups HACS (n = 3). (E) Protein expression of FTH1, FLT and CP of erastin and erastin + G1 groups HACS (n = 3). (F) Correlation of GPR30 with FTH1, FLT and CP using whole genome RNA sequencing data. *$P < 0.05$. Error bars represent SD.

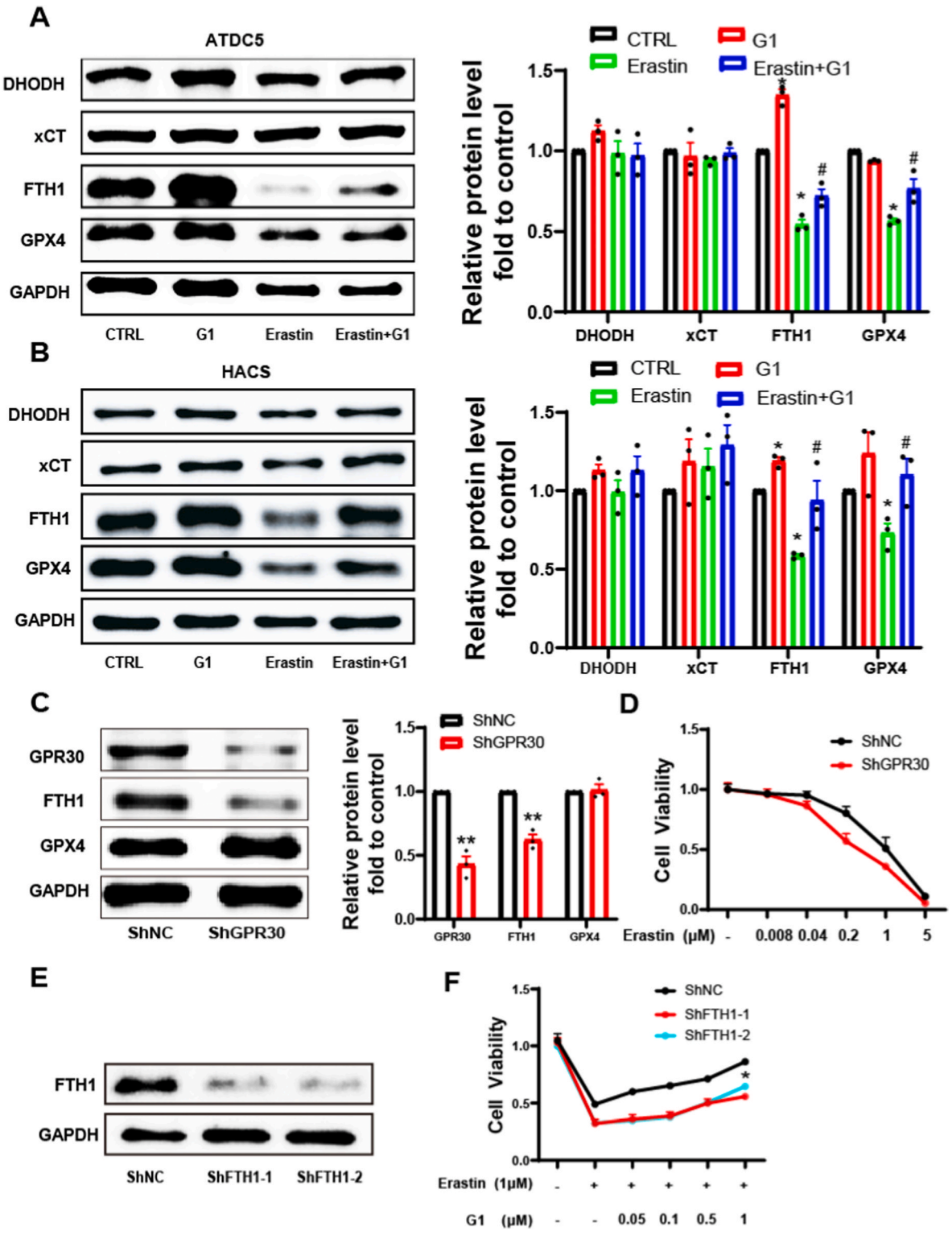

Figure 5. GPR30 activation exerted anti-ferroptosis effects by increasing FTH1 expression. (A) Protein expression of FTH1, GPX4, xCT and DHODH in ATDC5 cells treated with erastin and rescued via G1 for 24h analysed by Western blot (n = 3). (B) Protein expression of FTH1, GPX4, xCT and DHODH in HACS treated with erastin and rescued via G1 for 24h analysed by Western blot (n = 3). (C) The efficacy of GPR30 specific shRNA were measured by western blotting in ATDC5 cells. (D) Cell viability of ATDC5 -shNC and shGPR30 treated with different concentration erastin for 24 h measure by CCK8 (n = 3). (E) The efficacy of FTH1 specific shRNA were measured by western blotting in ATDC5 cells. (F) Cell viability of ATDC5 -shNC and shFTH1 treated with erastin and rescued via different concentration of G-1 for 24 h measure by CCK8 (n = 3). $^{*}P < 0.05$, $^{**}P < 0.01$ compared with control group. $^{\#}P < 0.05$ compared with erastin group. Error bars represent SD.

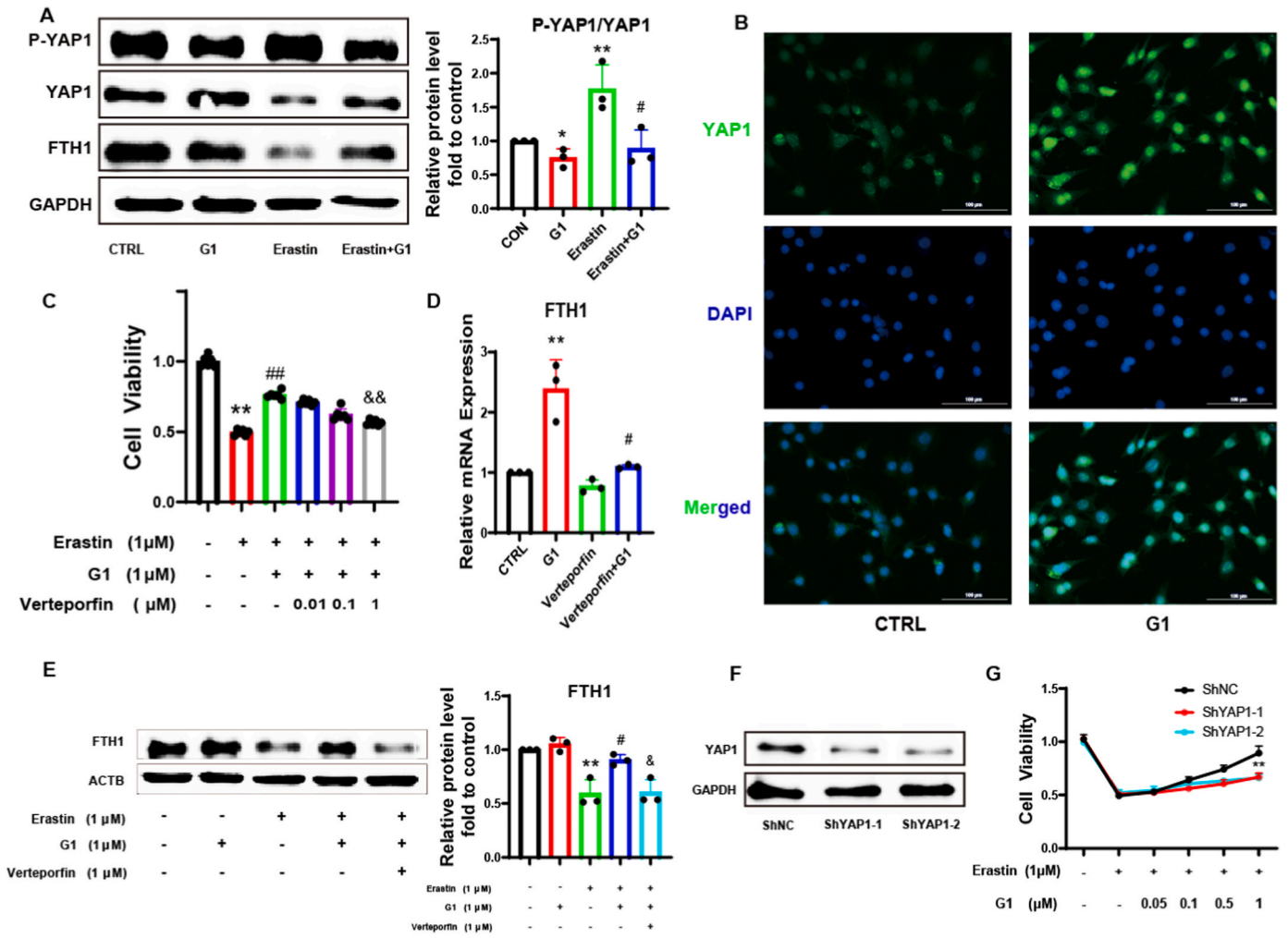

Figure 6. GPR30 activation inhibited YAP1 phosphorylation to regulate FTH1 transcription and protect against ferroptosis. (A) Protein expression of P-YAP1, YAP1, and FTH1 in ATDC5 cells treated with erastin and rescued via G1 for 24 h analysed by Western blot (n = 3). (B)The localization and expression of YAP1 in ATDC5 cells treated with G1 for 24 h were investigated by fluorescence (n = 3). (C) Cell viability of ATDC5 treated with erastin and rescued via G-1 and Verteporfin for 24 h measure by CCK8 (n = 6). (D) Quantitative PCR analysis of messenger RNA levels for FTH1 in ATDC5 treated with erastin and rescued via G-1 and Verteporfin for 24 h (n = 3). (E) Protein expression of FTH1 in ATDC5 cells treated with erastin and rescued via G1 and Verteporfin for 24h analysed by Western blot (n = 3). (F)The efficacy of YAP1 specific shRNA were measured by western blotting in ATDC5 cells. (F) Cell viability of ATDC5 -shNC and shYAP1 treated with erastin and rescued via different concentration of G-1 for 24 h measure by CCK8 (n = 3). $^{*}P < 0.05$, $^{**}P < 0.01$ compared with control group. $^{\#}P < 0.05$, $^{\#\#}P < 0.01$ compared with erastin group. $^{\&}P < 0.05$, $^{\&\&}P < 0.01$ compared with erastin + G1 group. Error bars represent SD.

significantly improved locomotion and pain in mice with OA in the late postoperative period, but they did not affect pain in the early postoperative period. Early postoperative pain is mainly due to surgery-induced damage, whereas late pain is mainly caused by OA. Therefore, we hypothesise that G1 exerts an indirect analgesic effect by slowing OA progression. Talwar et al. found that an oestrogen deficiency activates apoptosis in chondrocytes, leading to the onset and progression of OA [25]. Reports also suggest that GPR30 agonism attenuates mechanical stress-induced chondrocyte apoptosis [26]. Therefore, oestrogen may elicit protective effects on articular cartilage through oestrogen receptor agonism, including nuclear receptors and GPR30. We also found significantly lower GPR30 transcript and protein levels in osteoarthritic cartilage tissue than in normal cartilage tissue, but activating GPR30 significantly improved locomotion, reduced pain, and improved OARSI scores in osteoarthritic mice. Together, these results suggest that GPR30 has an essential role in OA.

Increasing evidence has shown that ferroptosis, characterised by the lethal accumulation of reactive iron and lipid peroxide, contributes to OA. Yao et al. first found that ferroptosis occurs in chondrocytes in inflammatory and iron overload conditions and that ferroptosis inhibition by intra-articular FER-1 injections prevented OA progression [17]. Furthermore, Miao et al. reported significantly lower GPX4 expression in the articular cartilage of patients with OA than in normal cartilage, and GPX4 regulated ferroptosis in OA and extracellular matrix degradation [27]. These studies are consistent with our results, where we found decreased GPX4 expression in osteoarthritic cartilage tissues compared to normal cartilage tissues using RNA sequencing. We also collected cartilage tissues from patients with OA, verifying decreased GPX4 expression in the cartilage tissues via immunohistochemical staining and western blotting. We also found significantly higher Fe^{2+} levels in cartilage tissue and joint fluid in patients with OA than in healthy participants, as well as peroxide metabolites accumulation in the cartilage tissue and decreased GPX4 expression in the OA mice compared to healthy mice, confirming that ferroptosis plays a key role in OA development.

Moreover, Liang et al. reported that ER agonism inhibits ferroptosis [15]. Similarly, we found that GPR30 has an important role in ferroptosis. GPR30 transcript and protein levels were significantly lower in osteoarthritic cartilage tissue than in normal cartilage tissue, negatively correlated with ferroptosis driver and marker genes, and positively

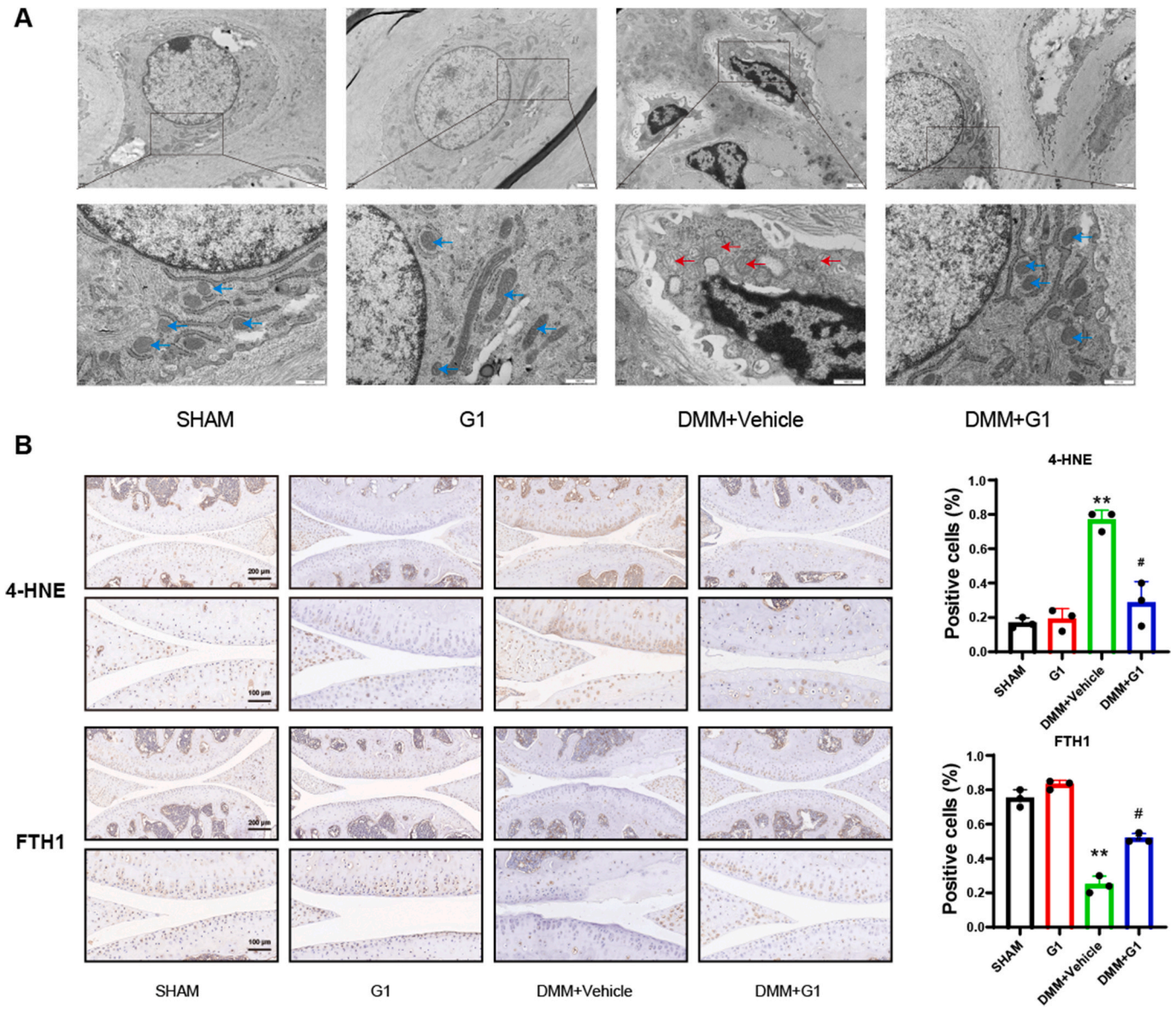

Figure 7. GPR30 activation inhibited ferroptosis and slowed down OA progression in mice. (A) Mitochondrial morphology of mice cartilage was observed using transmission electron microscopy (n = 3). (B) Immunohistochemistry assay with anti-4HNE and anti-FTH1 in mice cartilage (n = 3). $^{**}P < 0.01$ compared with sham group. $^{\#}P < 0.05$ compared with DMM + Vehicle group. Error bars represent SD.

correlated with ferroptosis suppressor genes. In addition, in vitro experiments demonstrated that G1 concentration-dependently ameliorated the erastin-induced decrease in chondrocyte viability and that G15 treatment or GPR30 silencing blocked its protective effect. Next, we evaluated changes in ferroptosis-related indicators when erastin-induced cell death was rescued by G1. Consequently, G1 treatment rescued the erastin-induced elevation of intracellular ROS, free ferrous ions, lipid peroxides, and MDA levels while restoring the chondrocyte mitochondrial membrane potential.

We also used proteomics to evaluate protein expression differences between the erastin + G1 and erastin-only groups, finding that the differentially expressed proteins were mainly associated with iron ion metabolism and were enriched in the ferroptosis pathway, further demonstrating that G1 acts primarily by inhibiting ferroptosis. FTH1 was the most significantly upregulated protein in the ferroptosis pathway, and GPR30 expression positively correlated with FTH1. In vivo and in vitro experiments also verified that agonising GPR30 increased FTH1 expression, consistent with a study by Qu et al. [22]. Furthermore, FTH1 catalyses the Fe^{2+} oxidation reaction, which is important for maintaining iron homeostasis and preventing ferroptosis [21]. Interestingly, GPR30 knockdown in ATDC5 cells simultaneously downregulated FTH1 expression but did not affect GPX4 expression, and the cells were more sensitive to ferroptosis after GPR30 (and subsequent FTH1) knockdown. These results suggest that GPR30 inhibits lipid peroxide production by increasing FTH1 levels and stabilising the intracellular iron pool, which minimises GSH depletion and GPX4 inactivation, exerting an anti-ferroptosis effect.

YAP1 is a transcriptional effector of the Hippo pathway and involved in various pathophysiological processes, including programmed cell death [28]. Phosphorylated YAP1 is retained in the cytoplasm by binding to 14-3-3 or is degraded by the ubiquitin-proteasome system. Dephosphorylated YAP1 localises to the nucleus, where it binds and activates TEAD family transcription factors, leading to cell proliferation, migration, and survival of target genes [29]. However, the role of YAP1 in articular cartilage remains controversial. Ying et al. reported that YAP1 knockdown maintained type II collagen expression and inhibited

cartilage degeneration in an OA model [30]. In contrast, Deng et al. suggested that YAP1 overexpression helped maintain articular cartilage integrity and reduced the inflammatory response within the joint, whereas a YAP1 deficiency led to cartilage destruction [29,31]. The Hippo/YAP1 signalling pathway also plays an important role in mediating the physiological functions of GPR30 in gene expression and cell proliferation [29]. Sun et al. reported decreased YAP expression in OA rat models, where GPR30 activation potentially increased YAP expression, inducing a shift in subcellular localisation from the cytoplasm to the nucleus, resulting in downregulation of mechanical stress-mediated signalling and apoptosis of chondrocytes [32]. Nonetheless, YAP1 is a key regulator of ferroptosis. Wu et al. found that YAP1 is a transcriptional stimulator of the ferroptosis-activating genes, acyl coenzyme A synthase long-chain family member 4 (i.e. ACSL4) and transferrin receptor [33]. In contrast, Zhang et al. found that YAP1 expression maintains ferritin transcript levels and protects against ferroptosis by stabilising the unstable intracellular iron pool [34]. Consistent with these findings, we found that GPR30 receptor agonism significantly increased FTH1 expression and correlated with Hippo pathway enrichment. In addition, GPR30 receptor agonism decreased the YAP1 phosphorylation level while increasing activated YAP1 expression, which increased translocation to the nucleus and thus increased FTH1 transcript and protein expression. However, YAP1 inhibitors reversed these effects. Nonetheless, the role of GPR30 in OA requires further validation using cartilage-specific knockout models.

In conclusion, GPR30 inhibits YAP1 phosphorylation, which regulates FTH1 expression and thus inhibits chondrocyte ferroptosis, which elicits protective effects against OA. We also demonstrate for the first time that GPR30 plays a key role in preventing ferroptosis. Thus, GPR30 could be an OA treatment target.

Fundings

The study was funded by the National Natural Science Foundation of China (NO. 82221001, NO. 32241007 and NO. 31972902), and partially supported by Shaanxi Province Key Industry Innovation Chain Project (Grant number 2023-ZDLSF-59).

Declaration of competing interest

A conflict of interest occurs when an individual's objectivity is potentially compromised by a desire for financial gain, prominence, professional advancement or a successful outcome. The Editors of the *Journal of Orthopaedic Translation* strive to ensure that what is published in the Journal is as balanced, objective and evidence-based as possible. Since it can be difficult to distinguish between an actual conflict of interest and a perceived conflict of interest, the Journal requires authors to disclose all and any potential conflicts of interest.

Acknowledgements

All persons who have made substantial contributions to the work reported in the manuscript (e.g., technical help, writing and editing assistance, general support), but who do not meet the criteria for authorship, are named in the Acknowledgements and have given us their written permission to be named. If we have not included an Acknowledgements, then that indicates that we have not received substantial contributions from non-authors.

Appendix A. Supplementary data

Supplementary data to this article can be found online at https://doi.org/10.1016/j.jot.2023.12.003.

References

[1] Rim YA, Nam Y, Ju JH. The role of chondrocyte hypertrophy and senescence in osteoarthritis initiation and progression. Int J Mol Sci 2020;21:2358. https://doi.org/10.3390/ijms21072358.
[2] Glyn-Jones S, Palmer AJ, Agricola R, Price AJ, Vincent TL, Weinans H, et al. Osteoarthritis. Lancet (London, England) (Lancet) 2015;386:376–87. https://doi.org/10.1016/S0140-6736(14)60802-3.
[3] Martel-Pelletier J, Barr AJ, Cicuttini FM, Conaghan PG, Cooper C, Goldring MB, et al. Osteoarthritis, Nature reviews. Disease primers. Nat Rev Dis Prim 2016;2:16072. https://doi.org/10.1038/nrdp.2016.72.
[4] Hunter DJ, Bierma-Zeinstra S. Osteoarthritis. Lancet (N AM ED) 2019;393:1745–59. https://doi.org/10.1016/S0140-6736(19)30417-9.
[5] Roman-Blas JA, Castaneda S, Largo R, Herrero-Beaumont G. Osteoarthritis associated with estrogen deficiency. Arthritis Res Ther 2009;11:241. https://doi.org/10.1186/ar2791.
[6] Chen R, Zhang M, Liu W, Chen H, Cai T, Xiong H, et al. Estrogen affects the negative feedback loop of PTENP1-miR200c to inhibit PTEN expression in the development of endometrioid endometrial carcinoma. Cell Death Dis 2018;10:4. https://doi.org/10.1038/s41419-018-1207-4.
[7] Ribeiro M, Sousa C, Rufino AT, Judas F, Mendes AF. Expression and function of the nonclassical estrogen receptor, GPR30, in human cartilage and chondrocytes. J Cell Physiol 2020;235:8486–94. https://doi.org/10.1002/jcp.29691.
[8] Wang XS, Yue J, Hu LN, Tian Z, Zhang K, Yang L, et al. Activation of G protein-coupled receptor 30 protects neurons by regulating autophagy in astrocytes. Glia 2020;68:27–43. https://doi.org/10.1002/glia.23697.
[9] Zhang Z, Qin P, Deng Y, Ma Z, Guo H, Guo H, et al. The novel estrogenic receptor GPR30 alleviates ischemic injury by inhibiting TLR4-mediated microglial inflammation. J Neuroinflammation 2018;15:206. https://doi.org/10.1186/s12974-018-1246-x.
[10] Prossnitz ER, Barton M. The G-protein-coupled estrogen receptor GPER in health and disease. Nat Rev Endocrinol 2011;7:715–26. https://doi.org/10.1038/nrendo.2011.122.
[11] Yang J, Hu S, Bian Y, Yao J, Wang D, Liu X, et al. Targeting cell death: pyroptosis, ferroptosis, apoptosis and necroptosis in osteoarthritis. Front Cell Dev Biol 2022;9:789948. https://doi.org/10.3389/fcell.2021.789948.
[12] Fischbacher A, von Sonntag C, Tc S. Hydroxyl radical yields in the Fenton process under various pH, ligand concentrations and hydrogen peroxide/Fe(II) ratios. Chemosphere 2017;182:738–44. https://doi.org/10.1016/j.chemosphere.2017.05.039.
[13] Zheng J, Conrad M. The metabolic underpinnings of ferroptosis. Cell Metab 2020;32:920–37. https://doi.org/10.1016/j.cmet.2020.10.011.
[14] Ru Q, Li Y, Xie W, Ding Y, Chen L, Xu G, et al. Fighting age-related orthopedic diseases: focusing on ferroptosis. Bone Res 2023;11:12. https://doi.org/10.1038/s41413-023-00247-y.
[15] Liang D, Feng Y, Zandkarimi F, Wang H, Zhang Z, Kim J, et al. Ferroptosis surveillance independent of GPX4 and differentially regulated by sex hormones. Jun 22 Cell 2023;186(13). https://doi.org/10.1016/j.cell.2023.05.003. 2748-2764.e22.
[16] Hsieh YC, Yu HP, Frink M, Suzuki T, Choudhry MA, Schwacha MG, et al. G protein-coupled receptor 30-dependent protein kinase A pathway is critical in nongenomic effects of estrogen in attenuating liver injury after trauma-hemorrhage. Am J Pathol 2007;170:1210–8. https://doi.org/10.2353/ajpath.2007.060883.
[17] Yao X, Sun K, Yu S, Luo J, Guo J, Lin J, et al. Chondrocyte ferroptosis contribute to the progression of osteoarthritis. J Orthop Transl 2021;27:33–43. https://doi.org/10.1016/j.jot.2020.09.006.
[18] Liang C, Zhu D, Xia W, Hong Z, Wang Q, Sun Y, et al. Inhibition of YAP by lenvatinib in endothelial cells increases blood pressure through ferroptosis. Biochim Biophys Acta (BBA) - Mol Basis Dis 2023;1869:166586. https://doi.org/10.1016/j.bbadis.2022.166586.
[19] Gao R, Kalathur R, Coto-Llerena M, Ercan C, Buechel D, Shuang S, et al. YAP/TAZ and ATF4 drive resistance to Sorafenib in hepatocellular carcinoma by preventing ferroptosis. EMBO Mol Med 2021;13:e14351. https://doi.org/10.15252/emmm.202114351.
[20] Imam Aliagan A, Madungwe NB, Tombo N, Feng Y, Bopassa JC. Chronic GPER1 activation protects against oxidative stress-induced cardiomyoblast death via preservation of mitochondrial integrity and deactivation of mammalian sterile-20-like kinase/yes-associated protein pathway. Front Endocrinol 2020;11:579161. https://doi.org/10.3389/fendo.2020.579161. 11.
[21] Tian Y, Lu J, Hao X, Li H, Zhang G, Liu X, et al. FTH1 inhibits ferroptosis through ferritinophagy in the 6-OHDA model of Parkinson's disease. Neurotherapeutics 2020;17:1796–812. https://doi.org/10.1007/s13311-020-00929-z.
[22] Qu Y, Li N, Xu M, Zhang D, Xie J, Wang J. Estrogen up-regulates iron transporters and iron storage protein through hypoxia inducible factor 1 alpha activation mediated by estrogen receptor β and G protein estrogen receptor in BV2 microglia cells. Neurochem Res 2022;47:3659–69. https://doi.org/10.1007/s11064-022-03658-1.
[23] Zhou X, Wang S, Wang Z, Feng X, Liu P, Lv X, et al. Estrogen regulates Hippo signaling via GPER in breast cancer. J Clin Invest 2015;125:2123–35. https://doi.org/10.1172/JCI79573.
[24] Xiao YP, Tian FM, Dai MW, Wang WY, Shao LT, Zhang L. Are estrogen-related drugs new alternatives for the management of osteoarthritis? Arthritis Res Ther 2016;18:151. https://doi.org/10.1186/s13075-016-1045-7.
[25] Talwar RM, Wong BS, Svoboda K, Harper RP. Effects of estrogen on chondrocyte proliferation and collagen synthesis in skeletally mature articular cartilage. J Oral

Maxillofac Surg: Off J Am Assoc Oral and Maxillofac Surg 2006;64:600–9. https://doi.org/10.1016/j.joms.2005.12.006.
[26] Sun Y, Leng P, Guo P, Gao H, Liu Y, Li C, et al. Protein coupled estrogen receptor attenuates mechanical stress-mediated apoptosis of chondrocyte in osteoarthritis via suppression of Piezo1. Mol Med 2021;27:96. https://doi.org/10.1186/s10020-021-00360-w.
[27] Miao Y, Chen Y, Xue F, Liu K, Zhu B, Gao J, et al. Contribution of ferroptosis and GPX4's dual functions to osteoarthritis progression. EBioMedicine 2022;76:103847. https://doi.org/10.1016/j.ebiom.2022.103847.
[28] Wang Y, Qiu S, Wang H, Cui J, Tian X, Miao Y, et al. Transcriptional repression of ferritin light chain increases ferroptosis sensitivity in lung adenocarcinoma. Front Cell Dev Biol 2021;9:719187. https://doi.org/10.3389/fcell.2021.719187.
[29] Deng Q, Jiang G, Wu Y, Li J, Liang W, Chen L, et al. GPER/Hippo-YAP signal is involved in Bisphenol S induced migration of triple negative breast cancer (TNBC) cells. J Hazard Mater 2018;355:1–9. https://doi.org/10.1016/j.jhazmat.2018.05.013.
[30] Ying J, Wang P, Zhang S, Xu T, Zhang L, Dong R, et al. Transforming growth factor-beta1 promotes articular cartilage repair through canonical Smad and Hippo pathways in bone mesenchymal stem cells. Life Sci 2018;192:84–90. https://doi.org/10.1016/j.lfs.2017.11.028.
[31] Deng Y, Lu J, Li W, Wu A, Zhang X, Tong W, et al. Reciprocal inhibition of YAP/TAZ and NF-κB regulates osteoarthritic cartilage degradation. Nat Commun 2018;9:4564. https://doi.org/10.1038/s41467-018-07022-2.
[32] Sun Y, Leng P, Guo P, Gao H, Liu Y, Li C, et al. Protein coupled estrogen receptor attenuates mechanical stress-mediated apoptosis of chondrocyte in osteoarthritis via suppression of Piezo1. Mol Med 2021;27:96. https://doi.org/10.1186/s10020-021-00360-w.
[33] Wu J, Minikes AM, Gao M, Bian H, Li Y, Stockwell BR, et al. Intercellular interaction dictates cancer cell ferroptosis via NF2–YAP signalling. Nature 2019;572:402–6. https://doi.org/10.1038/s41586-019-1426-6.
[34] Zhang X, Yu K, Ma L, Qian Z, Tian X, Miao Y, et al. Endogenous glutamate determines ferroptosis sensitivity via ADCY10-dependent YAP suppression in lung adenocarcinoma. Theranostics 2021;11:5650–74. https://doi.org/10.7150/thno.55482.